JOURNAL OF PETROLOGY | VOLUME 43 | NUMBER 2 | PAGES 000–000 | 2002

Adakite-like Lavas from Antisana Volcano (Ecuador): Evidence for Slab Melt Metasomatism Beneath the Andean Northern Volcanic Zone

ERWAN BOURDON[1,3]*, JEAN-PHILIPPE EISSEN[1], MICHEL MONZIER[2], CLAUDE ROBIN[2], HERVÉ MARTIN[2], JOSEPH COTTEN[3] AND MINARD L. HALL[4]

[1]IRD CENTRE DE BRETAGNE, BP 70, 29280 PLOUZANÉ CEDEX, FRANCE

[2]IRD ET UMR 6524, 5 RUE KESSLER, 63038 CLERMONT-FERRAND CEDEX, FRANCE

[3]UMR 6538, UNIVERSITÉ DE BRETAGNE OCCIDENTALE, BP 809, 29285 BREST CEDEX, FRANCE

[4]INSTITUTO GEOFÌSICO, EPN, APARTADO POSTAL 17-01 2759, QUITO, ECUADOR

RECEIVED APRIL 30, 2000; REVISED TYPESCRIPT ACCEPTED AUGUST 6, 2001

Extensive sampling of the Antisana volcano in Ecuador (Northern Volcanic Zone of the Andes) has revealed the presence of adakite-like rocks throughout the edifice, i.e. rocks with geochemical characteristics close, but not identical, to those of slab melts. Two main volcanic groups have been distinguished, characterized by two distinct evolutionary trends. The AND group, mostly composed of andesites, shows the clearest adakitic characteristics such as high La/Yb and Sr/Y ratios and low heavy rare earth element (HREE) contents. The CAK group, composed of high-K andesites and dacites, displays less pronounced adakitic-like characteristics. Although the more basic rocks of each group are difficult to distinguish on many geochemical diagrams, a geochemical study shows that the evolution of the AND and CAK groups is dominated by different petrogenetic processes. The isotopic characteristics of the CAK rocks suggest that evolution of this group is dominated by a limited assimilation–fractional crystallization process within the granitic continental basement of the cordillera. In the AND group, the abundances of incompatible elements, such as Nb or HREE, suggest that the series was produced by a partial melting process in a mantle rich in garnet, amphibole and/or clinopyroxene. Such a mantle source has been demonstrated (experimentally and by exhumed mantle xenoliths) to be produced in subduction zones where slab melts react with and metasomatize the mantle wedge. In Ecuador, magmas erupted in the Western Cordillera (trenchward relative to Antisana volcano) are true adakites, suggesting that slab melts can be responsible for the metasomatism of the mantle wedge beneath the NVZ in Ecuador. If mantle convection can drag down this modified mantle beneath Antisana volcano, destabilization of metasomatic amphibole at appropriate pressures in this modified garnetiferous mantle can adequately explain the formation and the geochemical features of Antisana lavas.

KEY WORDS: *subduction; adakite; metasomatism; Ecuador; AFC; Sr and Nd isotopes*

INTRODUCTION

It is widely accepted that magmas generated in subduction zones are generated in the depleted mantle wedge, the composition of which is modified and enriched by hydrous material fluxes released from the downgoing subducting plate (Tatsumi *et al.*, 1986; McCulloch & Gamble, 1991; Arculus, 1994). In the past few years, strong evidence has appeared that in some volcanic arcs (Kamchatka, Philippines, Aleutians) this enrichment can be due either to silicate melts or to aqueous fluids, or

*Corresponding author. Present address: IRD, Whymper 442 Y Coruña, A.P. 17-12-857, Quito, Ecuador. Fax: +593 2 504 020. E-mail: bourdon@ecnet.ec.

both (Yogodzinski *et al.*, 1994; Kepezhinskas *et al.*, 1996; Sajona *et al.*, 1996).

According to early magma genesis models (Ringwood, 1974; Wyllie & Sekine, 1982), slab melting was thought to be possible in subduction zones and offered an explanation for the genesis of the calc-alkaline series. Further, it was experimentally shown (Tatsumi *et al.*, 1986; Brenan *et al.*, 1994; Tatsumi & Kogiso, 1997) that partial melting of the mantle wedge metasomatized by hydrous fluids released from the downgoing slab could explain the main characteristics of subduction-related magmas and particularly the enrichment of large ion lithophile elements (LILE), Th, U and possibly light rare earth elements (LREE) over the high field strength elements (HFSE) and heavy REE (HREE).

At the same time, a peculiar type of orogenic rock was recognized, first in Adak Island (Aleutians; Kay, 1978) and then in 14 other volcanic arcs [see Maury *et al.* (1996) for a review]. These rocks, termed 'adakites' by Defant & Drummond (1990), display geochemical characterictics consistent with an origin as melts derived from the subducting oceanic crust.

The ever-growing number of locations where adakites are described shows that slab melting can no longer be considered as a rare phenomenon, requiring unusual P–T slab paths to occur (Peacock, 1990; Peacock *et al.*, 1994). It has even been shown that slab melts may possibly be involved in arc magma genesis without being necessarily emplaced at the surface (Maury *et al.*, 1998).

Here we present new geochemical data for an extensive sample set of rocks from Antisana volcano (Ecuador). These data suggest that magma genesis beneath this volcano is strongly influenced by silicate melts derived from the downgoing subducting plate. The potential magma source composition that would explain the geochemical trends displayed by Antisana rocks is also discussed.

ANTISANA VOLCANO: GEOTECTONIC SETTING AND MORPHOLOGICAL FEATURES

Subduction of the Nazca plate beaneath the South American plate is responsible for major Quaternary volcanism in three distinct provinces along the Andes (Fig. 1): the Northern Volcanic Zone (NVZ) in Colombia and Ecuador, the Central Volcanic Zone (CVZ) in Southern Peru and Northern Chile, and the Southern Volcanic Zone (SVZ) in Southern Chile (Thorpe *et al.*, 1982). In Ecuador (Fig. 1), Plio-Quaternary volcanism is represented by a great number of strato-volcanoes spanning >500 km of arc length. The width of the volcanic chain ranges from 120 km at 0°30'S to a lone volcano at its southern termination.

Antisana volcano is situated in the Eastern Cordillera at 0°30′S, at the latitude where the volcanic chain is broadest (Fig. 1). With an elevation of 5758 m, it is one of the largest Ecuadorian volcanoes. It is situated 50 km SE of Quito and much of its eruptive history remains unknown. It is constructed on the Cordillera Orientale Mesozoic to Quaternary volcano-sedimentary and metamorphic basement whose mean elevation ranges between 3000 and 4000 m. This basement is composed of old Tertiary volcanic rocks lying upon Mesozoic granites and metasedimentary rocks of the Loja division (Litherland *et al.*, 1994).

Antisana is a Quaternary stratovolcano built in at least two phases. The southeastern part represents the old edifice, which encompasses two-thirds of the volcano. It is composed of numerous volcanic breccia deposits, lava and pyroclastic flows whose eruptive history is totally unknown. Glacial erosion has strongly remodelled this old edifice. It seems that the old edifice activity terminated with at least two explosive events as indicated by both eastern and southern calderas, which are well expressed in topography (Fig. 1).

Antisana's northwestern flank is a young regular cone-shaped edifice representing about one-third of the total volcano. It is composed of numerous similar lava flows, probably originating from the summit. The extremely fresh appearance of the lava flows suggests that they were erupted in Holocene time. Few pyroclastic deposits have been recognized in this part of the volcano, suggesting a dominantly effusive recent activity.

Two important monogenetic lava flows seem related to the most recent activity of Antisana volcano; located a few kilometres away to the north from the main edifice, these are the Antisanilla and Potrerillos lava flows, which are, respectively, 10 and 15 km long. They erupted directly through fissures in the Cordillera Orientale basement and seem geochemically related to Antisana volcano. Both erupted in the eighteenth century.

Rocks analysed as part of this study were sampled from all around the volcanic edifice (see Bourdon *et al.*, 1999), including the hardly accessible eastern and southern slopes, and should therefore be representative of the overall Antisana magmatic history.

The region of the NVZ in which the Antisana volcano is located is characterized by a striking lack of intermediate depth seismicity (>60 km) in the subduction zone. Thus, the exact position of the slab under Antisana volcano is poorly constrained. Gutscher *et al.* (1999) proposed that there may be a 'flat slab' beneath this part of the NVZ, sustained by the buoyancy of the subducting Carnegie Ridge. According to those workers, the slab may be 100 km deep under Antisana volcano and only 80 km under the Cordillera Occidentale. A large uncertainity remains, however, on the exact location of the slab

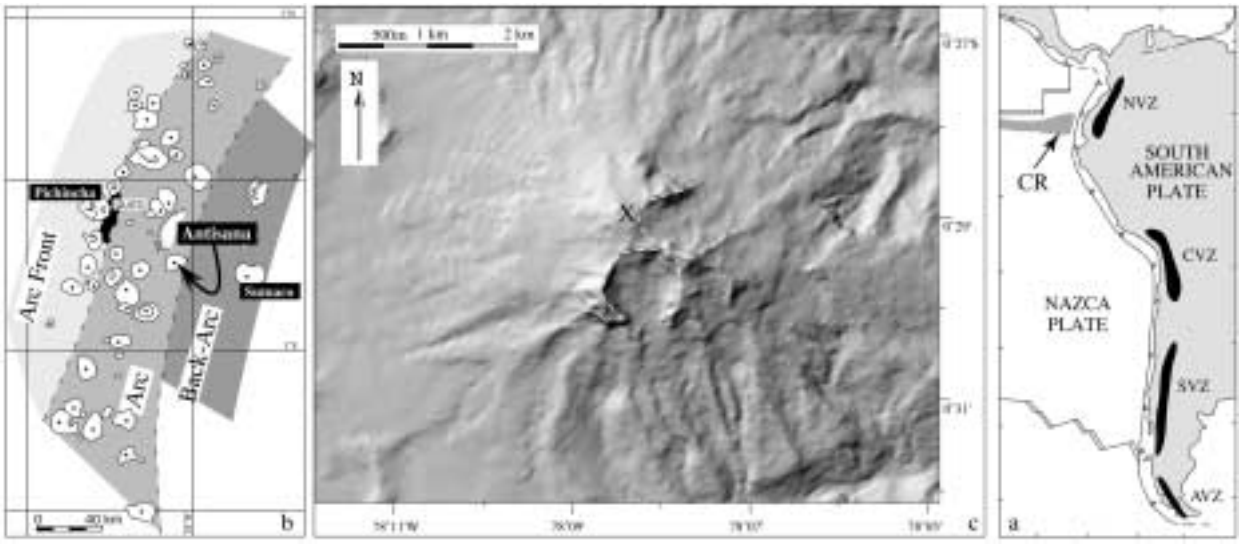

Fig. 1. (a) Location of the NVZ on the South American continent. CR, Carnegie Ridge. (b) Location of Antisana volcano in the NVZ of Ecuador. (c) Antisana topography seen in shaded relief illuminated from NW. X, edifice summit. White dashed lines are the limits of calderas.

beneath the central part of the Ecuadorian volcanic segment.

GEOCHEMISTRY OF ANTISANA LAVAS

Major and trace element abundances and Sr–Nd isotopic data for 15 representative lavas from Antisana volcano are listed in Table 1. Chemical compositions were obtained by inductively coupled plasma atomic emission spectrometry (ICP-AES) [except Rb, obtained by atomic absorption spectrometry (AAS)] at the Laboratoire de Pétrologie de l'Université de Bretagne Occidentale (Brest, France). Isotopic data were obtained at the Laboratoire de Géochimie Isotopique de l'Université de Clermont-Ferrand (France).

The Antisana lavas range in composition from very mafic andesites to highly evolved dacites. They can be divided into three types and two main groups. Rock classification is based on the K_2O vs SiO_2 diagram (Fig. 2a) modified from Peccerillo & Taylor (1976) as well as the Sr/Y vs Y diagram (Fig. 2b) and the MgO vs SiO_2 diagram (Fig. 2c). The distinction of two groups was made to emphasize the existence of two different evolutionary sequences, rather than two distinct petrogenetic groups, as the more basic rocks from both groups share many geochemical characteristics.

The AND group

This group is mostly composed of andesites (AND) together with two basic andesites displaying intermediate to high K_2O contents (1·5–2·7%). Their MgO contents range between 2·5% and 4·9%. This group has intermediate to high Na_2O contents (3·6–4·4%). The AND group mantle normalized trace element patterns display the typical enrichments (in LILE and LREE) and depletions (in HFSE) of subduction-related lavas, although these rocks do not generally display a negative anomaly in Ti (Fig. 3). In addition, they are characterized by very low HREE (e.g. Yb 0·77–1·04 ppm) and Y (10·4–13 ppm) contents, resulting in elevated Sr/Y (50–72) and La/Yb (21–39) ratios typical of adakites and experimentally simulated slab melts (e.g. Defant & Drummond, 1990; Sen & Dunn, 1994). Defant & Drummond (1990) proposed that adakites are the result of partial melting of subducting oceanic crust at the amphibolite–eclogite transition, before its dehydration. Among AND lavas, the more acid samples display the strongest adakitic characters such as higher Sr contents, and lower HREE and Y contents, as well as higher La/Yb and Sr/Y ratios.

Nevertheless, the AND lavas differ in many ways from typical adakites. For example, Al_2O_3 (16–17%) is not as high as expected for slab melts (commonly >17%) and K_2O contents are much higher (1·5–2·8%) than in typical adakites (usually <1·5%) resulting in low Na_2O/K_2O ratios (<2·5) untypical of slab melts. LILE concentrations in the AND group lavas are also much higher than in typical adakites (e.g. Rb 47–98 ppm). It is also necessary to emphasize that Antisana adakite-like lavas are basaltic to acid andesites whereas typical slab melts are thought to be andesitic to dacitic in composition (Defant & Drummond, 1990; Rapp & Watson, 1995). Lastly, no amphibole phenocryst was found in the mineralogy of these magmas although it is a common mineral phase

Table 1: Geochemical and Nd-Sr isotopic data for representative lavas from Antisana volcano

Sample:	ANT 8	ANT 10	ANT 14C	ANT 26	ANT 28	ANT 29C	ANT 32	ANT 36	ANT 37	ANT 46	ANT 47	ANT 54	ANT 60	ANT 61	ANT 62
Type:	CAK	CAK	CAK	AND	AND	CAK	CAK	CAK	AND	CAK	CAK	HAA	HAA	AND	AND
SiO_2	61·7	64·6	65	63	62·60	66·50	67·00	59·00	59·00	58·00	55·90	53·20	57·90	62·30	62·95
TiO_2	0·78	0·67	0·64	0·69	0·70	0·63	0·61	0·92	0·94	0·91	0·95	1·16	1·08	0·68	0·74
Al_2O_3	16	15·32	15·22	16·05	16·05	14·90	15·25	16·35	16·25	16·95	17·05	18·12	17·90	16·20	16·15
Fe_2O_3	5·85	4·94	4·69	5·50	5·67	4·27	4·18	7·20	6·75	7·40	7·91	8·55	7·40	5·42	5·46
MnO	0·09	0·07	0·07	0·08	0·08	0·06	0·06	0·10	0·09	0·09	0·10	0·12	0·11	0·08	0·08
MgO	3·02	2·46	2·23	2·83	2·84	1·28	1·30	4·01	3·30	3·73	4·88	3·62	2·45	2·89	2·52
CaO	5·47	4·3	3·95	5·08	4·80	3·14	3·25	6·14	5·94	6·27	6·33	7·20	5·81	5·14	4·97
Na_2O	4·31	4	3·98	4·07	3·70	3·88	4·00	3·94	4·21	4·05	3·94	3·91	4·42	4·09	4·25
K_2O	2·33	3·26	3·45	2·82	2·63	3·75	3·90	2·20	2·21	1·71	1·58	1·43	2·39	2·37	2·42
P_2O_5	0·24	0·21	0·18	0·20	0·21	0·20	0·19	0·28	0·30	0·26	0·27	0·33	0·34	0·22	0·24
LOI	−0·12	0·06	−0·08	−0·04	0·61	1·12	0·32	−0·13	0·28	0·37	0·58	1·91	−0·07	−0·02	−0·09
Total	99·67	99·89	99·33	100·28	99·89	99·73	100·06	100·01	99·27	99·74	99·49	99·55	99·73	99·37	99·69
Rb	62·5	128	139	98	96	165	170	71	67	43·5	36	26·5	66	77·5	62
Sr	776	655	535	638	597	436	455	714	790	716	749	870	735	722	732
Ba	846	940	925	1060	1110	1060	1130	825	920	728	708	694	960	1065	1130
Sc	11·3	9·6	9·1	9·8	10	5·9	6	12·9	10·7	13	14·5	13·8	13	11	9·8
V	138	110	105	122	130	87	79	166	158	167	180	205	169	129	123
Cr	56	48	47	73	79	15	17	108	90	94·0	174	13·5	4	99	32
Co	17·5	14	12	16	17	9	10	23	22	24·5	30	26	18	17	16
Ni	25	27·5	23	30	36	9	11	49	40	43	80	16	8·5	34	21
Y	11·7	15·6	15·1	10·4	10·8	17·3	17·7	15·1	12·7	12·5	13	16·5	19·3	11·1	10·6
Zr	111	147	147	158	156	252	262	164	171	133	133	140	189	138	125
Nb	8·7	11	11·6	7·7	8	13·4	13·2	9·3	9·7	6·6	7·35	9·4	10	6·6	8·1
La	26	35	35	30	27·5	40	40	29	29	23	22·5	24·5	29·5	30	29·5
Ce	48	64	64	53·5	51	76	76	57	58	45	44	49	57	53	55
Nd	24	29·5	29	24·5	23·5	34	32·5	28	29	24·5	24	26·5	30	25	25
Sm	4·3	4·9	4·9	4·3	4·2	5·8	5·9	5·35	5·3	4·7	4·7	5·3	5·7	4·4	4·2
Eu	1·15	1·09	1·05	1·05	1·07	1·12	1·07	1·33	1·35	1·28	1·29	1·51	1·51	1·12	1·17
Gd	3·6	3·9	4	3·4	3·4	4·6	4·35	4·3	4·1	4·2	3·9	4·85	4·7	3·35	3·4
Dy	2·3	2·7	2·8	2	2·15	3·1	3·05	2·85	2·6	2·6	2·65	3·3	3·6	2·15	2·15
Er	1·2	1·6	1·55	1·1	1·1	1·75	1·7	1·4	1·25	1·3	1·35	1·6	1·9	1·2	1·1
Yb	0·94	1·31	1·34	0·77	0·82	1·46	1·45	1·16	0·95	0·96	1·04	1·4	1·73	0·87	0·86
Th	8·9	19·1	20·4	13	12·5	24·5	24·8	10	9·2	5·5	4·7	4·7	9·1	10·3	9·9
$^{87}Sr/^{86}Sr$	0·704242	0·704398	0·704403	0·704411	0·704390	0·704383	0·704453	0·704310	0·704317	0·704376	0·704366	0·704507	0·704336	0·704365	0·704261
$^{143}Nd/^{144}Nd$	0·512763	0·512731	0·512735	0·512739	0·512745	0·512750	0·512726	0·512734	0·512749	0·512728	0·512736	0·512722	0·512725	0·512721	0·512759

Major element (in wt %) and trace element analyses (in ppm) were performed in Brest by ICP-AES following the method given by Cotten *et al.* (1995). Relative standard deviations are equal to or less than 2% and 5% for major and trace elements, respectively. Isotope ratios were determined at the Laboratoire de Geóchimie Isotopique de l'Université de Clermont-Ferrand. $^{87}Sr/^{86}Sr$ is corrected for mass fractionation by normalizing to $^{86}Sr/^{88}Sr = 0{\cdot}1194$ and given relative to an NBS SRM987 standard value of 0·710227 ($n = 12$). $^{143}Nd/^{144}Nd$ is corrected for mass fractionation by normalizing to $^{146}Nd/^{144}Nd = 0{\cdot}7219$ and given relative to a La Jolla Nd standard value of 0·511838 ($n = 8$).

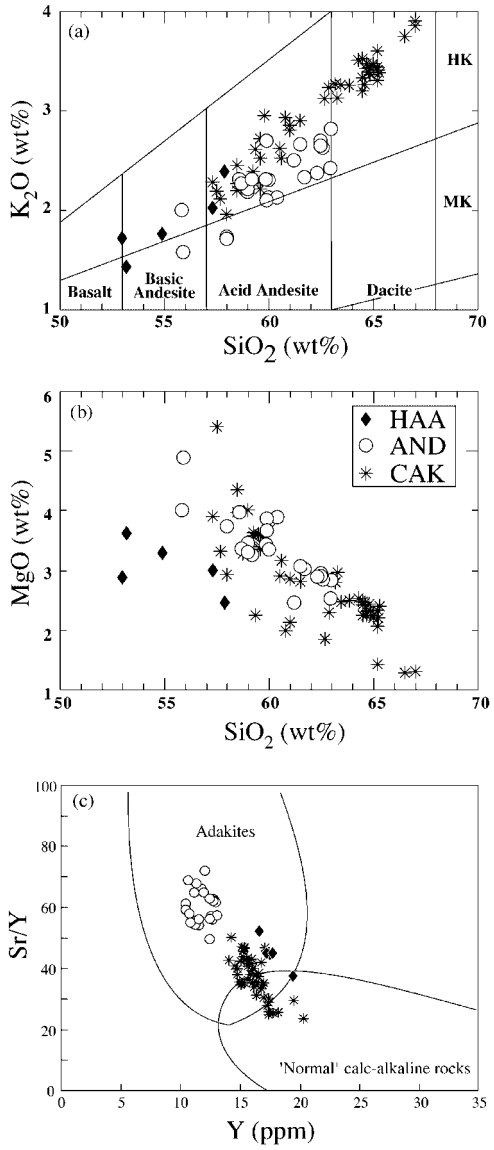

Fig. 2. (a) K_2O vs SiO_2 (wt %) classification diagram for orogenic magmas, modified from Peccerillo & Taylor (1976) showing the Antisana samples (circles, AND group; stars, CAK group; diamonds, HAAs from the AND group). (b) Diagram showing MgO variations vs SiO_2. (c) Sr/Y vs Y discrimination diagram between adakites and 'normal' calc-alkaline rocks (after Drummond & Defant, 1990).

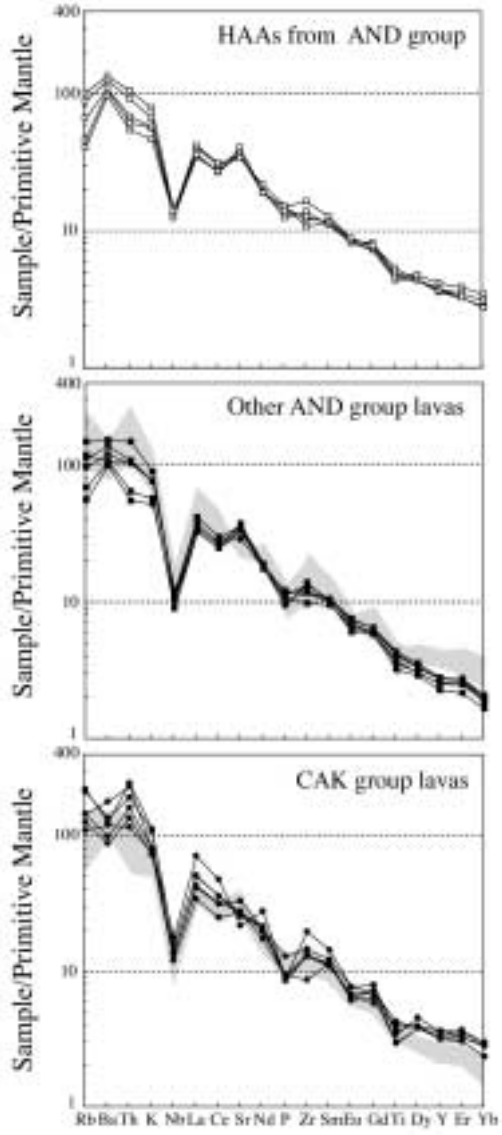

Fig. 3. Extended trace elements plots for representative lavas from the Antisana volcano normalized to primitive mantle of Sun & McDonough (1989). In the AND plot, the shaded area corresponds to rocks from CAK group, and the reverse for the CAK plot.

in typical adakites in many arc environments where such magmas are erupted (Defant & Drummond, 1990; Maury *et al.*, 1996).

Five samples of a peculiar type of lava were also included in the AND group. These rocks are high-Al andesites (HAAs), which display unusually low MgO contents (2·4–3·6%) for such 'basic' rocks (53 < SiO_2 <58%). They have the highest TiO_2 (0·97–1·16%) and Al_2O_3 (17–18·2%) contents among Antisana rocks (Table 1). They also have intermediate to high Na_2O (3·7–4·4%) and K_2O (1·43–2·49%) contents. Along with their low MgO concentrations, their *mg*-number values are unusually low (40–46). Lastly, hypersthene is commonly found in their norm. The geochemical characteristics of these rocks are very close to those of low-MgO high-aluminium basalts and basaltic andesites described by previous workers (e.g. Kuno, 1960). These HAAs were included in the AND group because of the numerous geochemical similarities with the other rocks from the group and also because they can be directly related to these by a simple fractional crystallization process.

Under water-saturated conditions at crustal levels (2 kbar), Sisson (1991) successfully produced a low-MgO HAB from a high-MgO parent by fractional crystallization. Under hydrous conditions, the appearance of plagioclase as an early phase is suppressed and the derivative lavas remain high in Al_2O_3. Sisson & Grove (1993) further showed experimentally that low-MgO HABs could have existed as liquids within the crust with H_2O contents of 4% or higher at temperatures <1100°C. Degassing at shallow depth would force them to grow phenocrysts, and provide an explanation for the usual abundant phenocryst nature of low-MgO HABs. The results of Sisson & Grove (1993) support models in which H_2O carried and released by the subducting slab flows through the mantle and initiates melting (e.g. Tatsumi, 1986), but this necessitates parental magmas with particularly high H_2O contents.

We calculated that adding back in only 7·5% of a two-pyroxene–olivine assemblage is sufficient to raise MgO content of HAA ANT 53A from 2·45% to 4·2% without significantly modifying other major and trace elements (except Al_2O_3, Na_2O and compatible trace elements; Fig. 4). This raises the Antisana HAA *mg*-number from 40–46 to 51–54, very similar to the *mg*-number of other basic rocks from the AND group. Therefore, it is conceivable that the HAAs can be derived from more magnesian lavas with major and trace element abundances close to those of the most basic rocks of the AND group. This would suggest, following Sisson & Grove (1993), that these magmas were particularly H_2O rich. This 'fractionation model' for deriving HAAs from a more mafic parent is weakened by the lack of examples of this mafic parent in our sample set, although this was perhaps not extensive enough to discover this mafic parental magma. It is also important to note that such a derivation has also been proposed for high-aluminium basalts from the Southern Andes and Kamchatka (Lopez-Escobar *et al.*, 1977; Hochstaedter *et al.*, 1996). Including the Antisana HAAs in the AND group defines a coherent group, requiring slight (<10%) mafic mineral fractionation to produce the HAAs from the most primitive magmas. Strong relations between the two rock types are also obvious in trace or major element ratio variation diagrams, in which they always define coherent arrays (except for compatible trace elements).

The CAK group

The second group consists of highly potassic calc-alkaline andesites and dacites (CAK) with K_2O contents up to 4%. The major element characteristics of the CAK group are very similar to those of the AND group at low SiO_2 contents although K_2O is slightly higher and Na_2O lower. The CAK group is differentiated from the AND group mainly on the basis of a Sr/Y vs Y diagram (Fig. 2c) and Yb contents (Fig. 4). The CAK group has lower Sr/Y ratios with higher absolute concentrations of Y and HREE, and is thus closer to a 'normal' calc-alkaline series.

The CAK group also displays characteristic features of subduction-related lavas (e.g. high concentrations of LILE, low HFSE contents). Unlike the AND group, however, they also display a negative anomaly in TiO_2 (Fig. 3). Although HREE and Y concentrations are higher than those of the AND group, these values are unusually low for 'normal' calc-alkaline rocks. This feature results in high La/Yb ratios (20–31) in this group. For the more 'basic' samples, it is very difficult to distinguish between the AND and CAK groups (Fig. 4) as the less silicic andesites of both groups share many common geochemical characteristics in several discrimination diagrams (see below).

The CAK group is less homogeneous than the AND group, the latter showing well-defined geochemical trends. There is much scattering in trace element concentrations (e.g. Yb, Fig. 4) among this group. Unlike the AND group, it is more difficult to discuss the petrogenesis of CAK as a single series. Also, unlike the AND group, the CAK group displays rather constant La/Nb ratios ($\sim$3).

PETROGRAPHIC CHARACTERISTICS

The Antisana rocks are characterized by a surprisingly homogeneous mineralogy comprising plagioclase, clino- and orthopyroxene, as well as ilmenite and magnetite. In contrast to most calc-alkaline series, amphibole is absent, although it could have existed in some dacites from the CAK group (see below). Antisana lavas are generally highly porphyritic (often >40% modal phenocryst content).

The AND group

Among the AND group, HAAs are characterized by a trachytic groundmass always dominated by plagioclase laths. These rocks can be extremely rich in plagioclase phenocrysts, sometimes representing >50% of the mode. They display the most anorthitic compositions among the Antisana rocks (up to An_{72}). Crystals cores ($An_{53–72}$) and rims ($An_{50–71}$) can be equally rich in anorthite, although they generally display normal zoning. Magnetite is present as rounded crystals and no ilmenite was found. Despite the fairly mafic geochemical characteristics of these rocks, no olivine phenocrysts were observed. Both clinopyroxene (augite) and orthopyroxene (bronzite) occur, although the former is dominant.

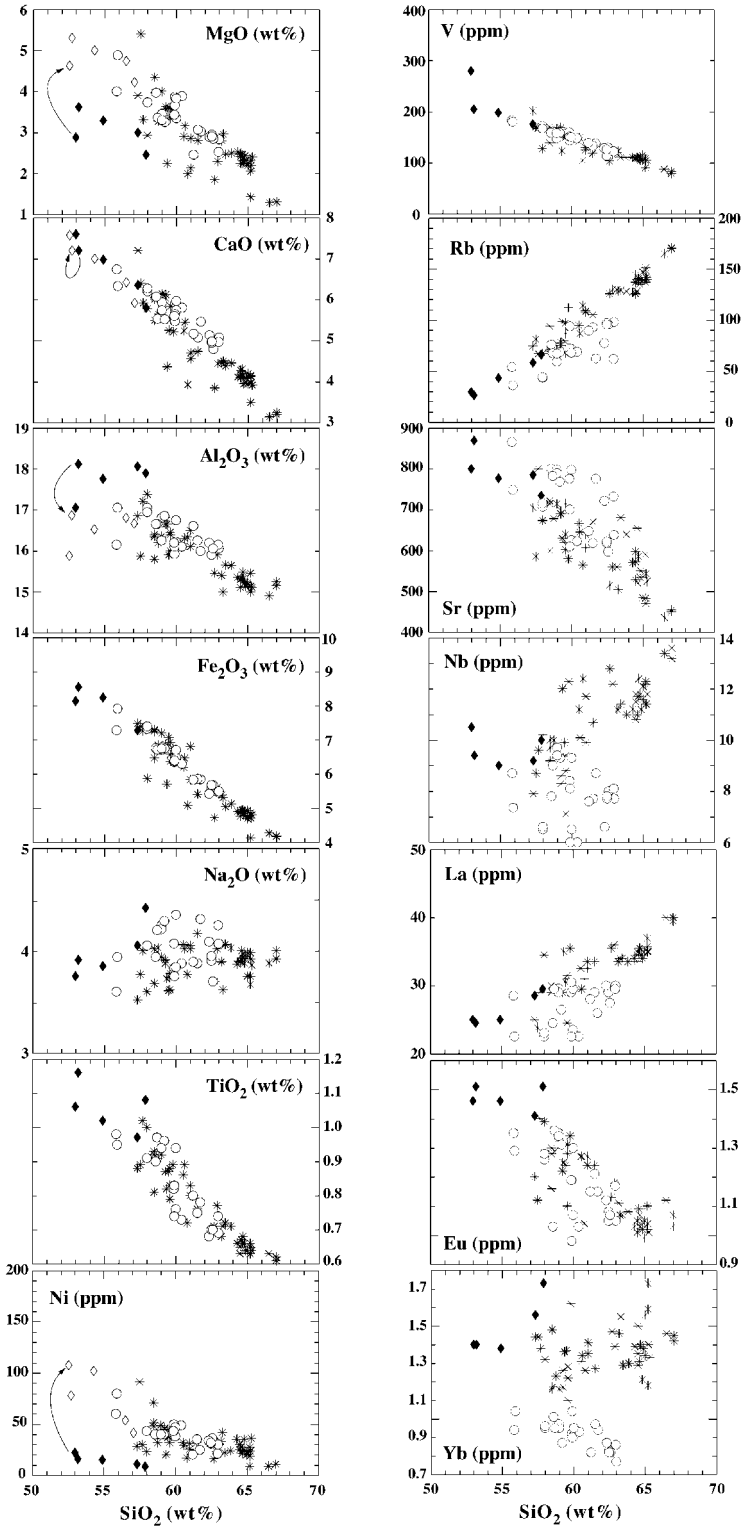

Fig. 4. Harker variation diagrams showing the major and trace element variations in the Antisana lavas. Same symbols as in Fig. 2. ◇, fractionation-corrected HAAs (see text). In subsequent figures, the entire AND group (including HAAs) are plotted with the same symbol.

Other rocks from the AND group are mostly porphyritic massive lavas. Plagioclase is slightly less anorthite rich than that in the HAAs and often displays reversed zoning with similar rims ($An_{45–68}$) and cores ($An_{49–63}$). In common with the HAAs, clinopyroxene phenocrysts are mostly augite, with subordinate diopside. The Ca-poor pyroxene is normally bronzite, although one hypersthene crystal was found. The AND group lavas (excluding the HAAs) are rich in magnetite and ilmenite. No amphibole was found in any these lavas, although this mineral phase is common, and characteristic of typical adakites (Defant & Drummond, 1990; Maury *et al.*, 1996).

Among the AND group, ANT 8, which was sampled from the monogenetic Antisanilla lava flow, displays distinctive petrological characteristics suggesting substantial interaction with the Cordillera Orientale basement. One olivine ($Fo_{75–80}$) and corroded quartz crystals were found in this sample, suggesting that these are xenocrysts. Also, some plagioclase crystals display unusually low anorthite contents ($An_{20–22}$) compared with the bulk of the Antisana lavas.

The CAK group

CAK group andesites and dacites contain the most anorthite-poor plagioclases displaying either normal or reverse zoning. Andesites and dacites display similar core and rim compositions, with plagioclase rims in the dacites displaying the lowest An contents (down to An_{26}). As in the AND group, the dominant Ca-rich pyroxene is augite with some subordinate diopside. Concerning the Ca-poor pyroxene, the CAK andesites are characterized mostly by bronzite, whereas hypersthene is dominant in the dacites, with some rare crystals of enstatite and pigeonite. These lavas are also rich in Fe–Ti oxides (titanomagnetite and ilmenite).

CAK dacites are rich in clusters of plagioclase–pyroxene–magnetite assemblages that sometimes seem to mimic former mineral 'ghosts', suggesting amphibole destabilization. A single microphenocryst of amphibole (among all the Antisana rocks) was found in one of these clusters. The total absence of amphibole in well-formed crystals suggests that this destabilization is not a directly pre-eruptive or syn-eruptive reaction but that it was a long and progressive reaction. This would mean that CAK magmas would have been pooled for a long time in the magma chamber before eruption.

ISOTOPIC RESULTS

Fifteen Nd–Sr isotopic measurements (Table 1) were carried out on Antisana volcanic rocks, spanning the entire range of rock composition (from low-Mg basic andesites to evolved dacites). These data are presented in Fig. 5 together with our unpublished analytical data from the NVZ. It appears that the Nd–Sr isotope composition is strikingly homogeneous in all the Antisana rocks ($^{87}Sr/^{86}Sr$ = 0·7042–0·7045, $^{143}Nd/^{144}Nd$ = 0·512721–0·512763) despite the variability in incompatible trace elements ratios and SiO_2 contents.

These new isotope data lie in the range previously defined for the Quaternary volcanic rocks of the NVZ, although Harmon *et al.* (1984) analysed two samples from the Puñalica eruptive centre (near Chimborazo volcano) with a slightly less radiogenic Sr isotope composition ($^{87}Sr/^{86}Sr$ <0·7039). Data from the Galápagos Islands, Galápagos Spreading Centre and the East Pacific Rise MORB and the CVZ are also shown for comparison in Fig. 5.

Within the NVZ, the Antisana rocks display the more radiogenic Sr and less radiogenic Nd isotope ratios typical of the Eastern Cordillera of Ecuador Quaternary magmas. The AND and CAK groups are indistinguishable on the basis of their Nd–Sr isotope characteristics. The CAK samples display a limited range of Sr isotope compositions, which are correlated with the Rb/Sr ratio, suggesting the involvement of assimilation–fractional crystallization (AFC) processes in the petrogenesis of the magmas (see below). Homogeneity of isotopic ratios suggests that the petrogenetic evolution of Antisana rocks is not dominated by the increasing contribution of contaminant derived from the downgoing slab [altered mid-ocean ridge basalt (MORB) or sediments] or by the continental crust. This also suggests that the parental magmas of both AND and CAK groups are chemically closer than previously expected based on the trace element data, and could be generated by partial melting of mantle sources of different mineralogical composition rather than different geochemical composition.

The MORB-like isotopic signature of adakites is one of their important characteristics worldwide (Defant *et al.*, 1992; Yogodzinski *et al.*, 1994; Kepezhinskas *et al.*, 1996). This characteristic has been attributed to the direct derivation of adakitic magmas from the subducted slab and the absence of a significant sedimentary component in their petrogenesis (e.g. Drummond *et al.*, 1996). None the less, many adakites in some arc settings also display a slightly more radiogenic Sr isotope signature than typical MORB (e.g. Pinatubo, Philippines; Central America). The Antisana rocks display a more radiogenic Sr signature compared with typical adakites. Also, they are slightly more radiogenic than rocks from the Western Cordillera. This radiogenic signature could be a consequence of some crustal assimilation of the Eastern Ecuadorian continental basement.

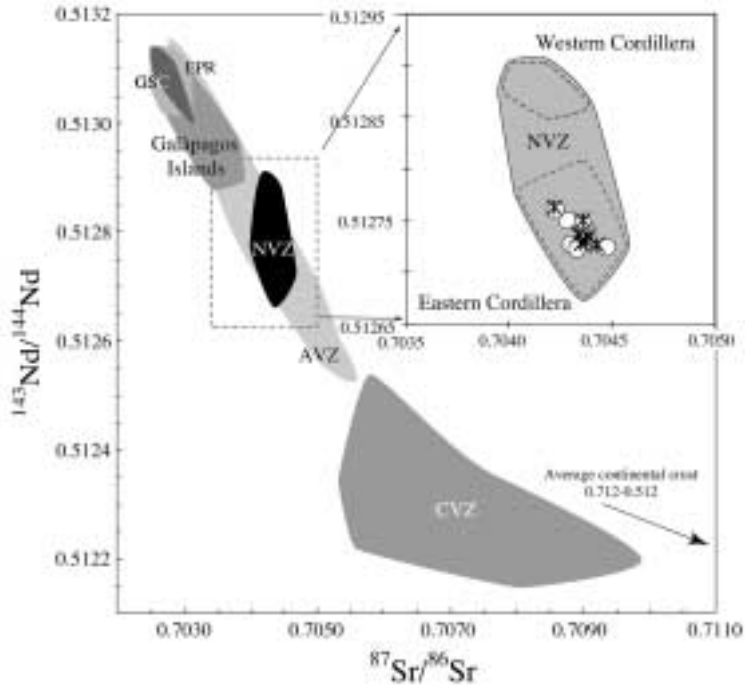

Fig. 5. $^{143}Nd/^{144}Nd$ vs $^{87}Sr/^{86}Sr$ diagrams. Comparison of Antisana rock data with those of the NVZ in Ecuador (E. Bourdon, unpublished data, 1999). Fields of isotopic data for the Galápagos Islands, Galápagos Spreading Centre (GSC) and the East Pacific Rise (EPR) (White *et al.*, 1993, and references therein), the Austral Volcanic Zone (AVZ) (Stern *et al.*, 1984; Stern & Kilian, 1996), and the Central Volcanic Zone (CVZ) (Hawkesworth *et al.*, 1982; James, 1982; Harmon *et al.*, 1984; Davidson *et al.*, 1990) are also shown. Circles, AND group; stars, CAK group.

TECTONIC SETTING OF MAGMA PRODUCTION AT ANTISANA VOLCANO

Peacock *et al.* (1994) calculated that, for a 'normal' thermal regime, subducted oceanic crust older than 5 Ma cannot melt because at pressures >2 GPa the corresponding geotherms do not crosscut the MORB solidus (Wyllie & Wolf, 1993). Nevertheless, the geochemical characteristics of adakitic magmas strongly suggest that they do indeed represent melts of oceanic basalts metamorphosed in the garnet-amphibolite facies (Defant & Drummond, 1990; Drummond & Defant, 1990). Melting experiments on garnet amphibolites at 800–1025°C under pressures of 1·5–2 GPa demonstrate that partial melts very similar to natural adakites can be generated (Rapp *et al.*, 1991; Sen & Dunn, 1994). These *P–T* conditions correspond to a thermal regime hotter than in 'normal' subduction zones and the resulting magmas would be erupted closer to the trench than 'normal' calc-alkaline lavas. On the basis of thermal models, Peacock *et al.* (1994) summarized the specific geodynamical conditions necessary to allow slab melting. These are: (1) high shear stresses (>100 MPa); (2) subduction of very young (<5 Ma) oceanic lithosphere; (3) an early stage of subduction. Peacock *et al.* (1994) admitted, however, that if the angle of subduction chosen for the model was reduced, the limiting age for slab melting could rise to 10 Ma. According to the geodynamic setting of present-day adakites (Defant & Drummond, 1990), it has also been proposed that they may be produced through melting of oceanic crust <25 Ma old or previously subducted oceanic crust (Saunders *et al.*, 1987). Alternatively, Atherton & Petford (1993) suggested that Na-rich magmas, very similar to adakites, could be produced by undersaturated partial melting of underplated mafic lower crust.

In the case of Ecuador, the present-day convergence rate between the Nazca plate and the Andean block is estimated to be 7 cm/yr (Gutscher *et al.*, 1999) and the role of high shear stress is thus thought to be negligible. The age of the oceanic crust currently being subducted under this part of South America is between 12 and 22 Ma, corresponding to the limits for possible adakite generation (Defant & Drummond, 1990). Another source of complexity is the subduction, at this location, of the aseismic Carnegie Ridge, originally produced by the passage of the Nazca plate over the Galápagos hotspot. In addition, particularly high heat flow values have been reported offshore Ecuador (Van Andel *et al.*, 1971).

The volcanic zone clearly displays a progressive broadening from Colombia to Ecuador where the Carnegie

Ridge is subducted. In Colombia, the NVZ is represented by a single chain of volcanoes whereas in Ecuador it is composed of at least two volcanic lineaments. The western volcanic chain is closer to the trench than the volcanic front in Colombia (~240 km instead of 320 km; Gutscher *et al.*, 1999). This suggests that magmas in the Western Cordillera are erupted in a fore-arc position, compared with the Colombian volcanic arc, similar to the tectonic setting of 'normal' adakites.

New geochemical data for volcanic rocks erupted in the Western Cordillera strongly suggest that typical adakites are erupted in this part of the volcanic arc (Bourdon *et al.*, 2001). Adakite genesis under the Western Cordillera is also in good agreement with the 80 km estimated depth of the Benioff zone beneath this part of the arc (Gutscher *et al.*, 1999), but it seems too deep beneath the Cordillera Occidentale and Antisana volcano (~100 km; Gutscher *et al.*, 1999).

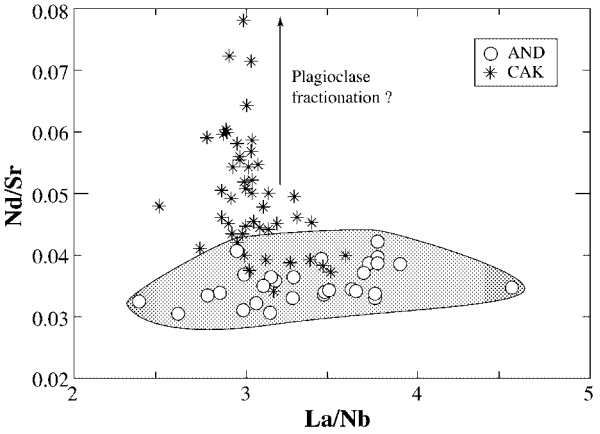

Fig. 6. Nd/Sr vs La/Nb diagram. Increasing Nd/Sr ratio among CAK group suggests plagioclase fractionation. The AND group includes HAAs.

DISCUSSION: ORIGIN AND EVOLUTION OF ADAKITIC-LIKE LAVAS FROM ANTISANA VOLCANO

As both the AND and CAK groups were erupted more or less simultaneously (Bourdon *et al.*, 1999), one could envision a petrogenetic relationship. In many geochemical variation diagrams (see Fig. 4), however, it is clear that both groups define divergent geochemical trends that are difficult to relate to one another. For example, the CAK group displays increasing SiO_2 contents correlated with increasing Yb concentrations, whereas, in the AND group, Yb concentrations decrease. Nevertheless, both trends tend to originate in a common parental magma composition.

Fractional crystallization within the AND and CAK groups

The AND group (including high-Al andesites) is characterized by unusual geochemical trends. For example, SiO_2 enrichment is correlated with decreasing Nb and HREE contents (Fig. 4) whereas the inverse is generally observed in most calc-alkaline series. Fractional crystallization of typical low-pressure phases is unable to explain such trends.

Amphibole fractionation might theoretically have been responsible for the observed trends (increasing La/Yb with decreasing Yb, decreasing Nb), but $K_d^{Nb/amph}$ (~1) and $K_d^{Yb/amph}$ (1·5–2) would necessitate fractionation of unrealistically large amounts of amphibole. The lack of amphibole phenocrysts in AND group lavas argues against significant fractionation of this mineral. Moreover, if amphibole fractionation was responsible for Yb depletion, it would decrease Gd (middle REE; MREE) more efficiently than is observed. There are only small variations in Zr/TiO_2 ratios in the AND group, which rules out fractionation of zircon as being responsible for the trace element distribution.

Obviously, some fractional crystallization must have occurred in the petrogenesis of the AND group (leading to some scattering in trace element diagrams, and variation of the *mg*-number), but it is not the dominant petrogenetic process that can be used to explain geochemical variations in the series. For example, in the Nd/Sr vs La/Nb diagram (Fig. 6), it is clearly shown that plagioclase fractionation plays a minor role, as the Nd/Sr ratio remains constant whereas the La/Nb ratio shows a wide range of variation.

Fractional crystallization seems to play a more important role within the CAK group rocks. This is, however, difficult to model because of the strong geochemical heterogeneity of this group. Nevertheless, in Fig. 6, the evolution of the CAK group displays a strong variation in the Nd/Sr ratio whereas the La/Nb ratio remains constant. This suggests that the petrogenetic evolution of the CAK group is dominated by fractional crystallization with significant amounts of plagioclase ($D_{Sr} = 2$). Nevertheless, the Nd–Sr isotopic variation within the group suggests that another process is occurring, probably AFC (see below).

AFC and deep crustal contamination processes

AFC processes

It has long been recognized that crustal contamination plays a minor role in the petrogenesis of lavas from the Northern Volcanic Zone in Ecuador (Thorpe *et al.*, 1982;

Table 2: Rb, Sr and Th (ppm), and $^{87}Sr/^{86}Sr$ data used in the AFC calculations

	Rb	Sr	Th	$^{87}Sr/^{86}Sr$
Starting magma*	71	714	10	0·704310
Assimilant†	150	100	13	0·720000

*Equivalent to ANT 36.
†Equivalent to the Tres Lagunas Granite complex [mean data taken from Litherland *et al.* (1994)].

Harmon *et al.*; 1984; James & Murcia, 1984) relative to the Central Volcanic Zone. Barragan *et al.* (1998) have recently estimated that the amount of crustal assimilation in the petrogenesis of the Antisana volcanic rocks is 8% by simple bulk mixing between a primitive mantle-derived magma and a typical continental crustal component. Here, we provide a full Nd–Sr isotopic dataset from the least to the most evolved Antisana rocks, providing an opportunity to constrain more precisely the degree of crustal assimilation.

The Antisana volcano is built upon the Mesozoic to Cenozoic Loja division of the Cordillera Real basement consisting of metasedimentary rocks and granites. Antisana is precisely situated above a Triassic granitic complex (Geological Map of Ecuador, IGM, 1993), analogous to the southernmost 'Tres Lagunas granite complex' (Litherland *et al.*, 1994).

In Fig. 7, good correlations are observed between $^{87}Sr/^{86}Sr$ and Th concentration and Rb/Sr ratio within the CAK group. Among this group, ANT 36 was considered as the most primitive lava composition and we use this as a parental magma to evaluate AFC processes within this series. The starting magma (ANT 36) and crustal contaminant (considered to be an equivalent of the Tres Lagunas granite) characteristics are given in Table 2. D_{Sr} is assumed to be constant and equal to 1·1 and D_{Rb} = 0·1, realistic values for the range from basaltic andesite to dacite (e.g. DePaolo, 1981; Gill, 1981). In both the $^{87}Sr/^{86}Sr$ vs Rb/Sr and Th diagrams, the data can be modelled by an AFC process with r values between 0·04 and 0·05. The calculated percentage of assimilated Triassic crust varies between 2·2 and a maximum of 4·5%. These values confirm that crustal assimilation is not a dominant process in the evolution of NVZ volcanic rocks, but on the other hand, it shows that AFC processes can perfectly explain some of the isotopic variations within the Antisana rocks.

Although the majority of the AND group do not show any correlation that could be associated with AFC processes, some rocks of this group seem to display a

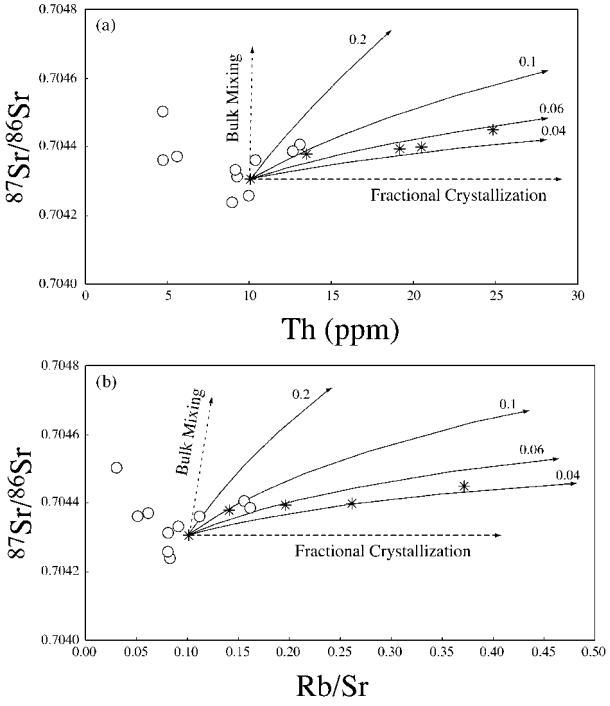

Fig. 7. AFC model curves (continuous lines) for different $r$values (ratio of mass assimilated to mass fractionated) in $^{87}Sr/^{86}Sr$ vs Th (a) and $^{87}Sr/^{86}Sr$ vs Rb/Sr (b) diagrams. In both diagrams, the correlation between $^{87}Sr/^{86}Sr$ and Th or Rb/Sr, respectively, should be noted. The CAK rock ANT 36 is considered as the starting magma. Trends for simple fractional crystallization or bulk mixing (dashed lines) are also illustrated. Same symbols as in Fig. 6.

similar behaviour to the CAK group (i.e. increasing Rb/Sr ratio correlated with $^{87}Sr/^{86}Sr$ ratio; Fig. 7). Nevertheless, this variation, if significant, corresponds to a very low percentage of assimilation. This feature suggests that some (or maybe all) of the AND group rocks could have been affected by minor amounts of upper-crustal contamination. One of the high-Al andesites of the AND group rocks also displays the highest $^{87}Sr/^{86}Sr$ and lowest $^{144}Nd/^{143}Nd$ ratios, suggesting that it also experienced some contamination.

Deep crustal contamination

Atherton & Petford (1993) showed that rocks from the Cordillera Blanca batholith display adakitic characteristics such as low Yb, high Sr and high SiO_2 contents. Several workers have suggested that similar characteristics in Quaternary lavas from CVZ volcanoes could be the result of partial melting within the thick garnetiferous lower continental crust of the Central Andes (e.g. Hildreth & Moorbath, 1988; Feeley & Hacker, 1995). The AND group, however, exhibits intriguingly rather high and constant *mg*-number that cannot be related to melting of the lower crust; such melts would be expected to have low *mg*-number (Yogodzinski & Kelemen, 1998). Also,

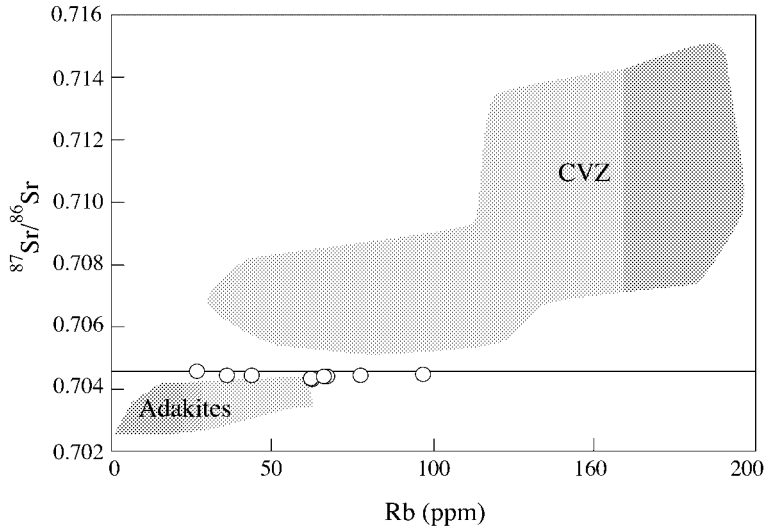

Fig. 8. $^{87}Sr/^{86}Sr$ vs Rb for Cenozoic adakites and CVZ data from the Andes compared with Antisana AND group data. (See explanation in the text.) Figure modified from Drummond *et al.* (1996).

in Fig. 8 the AND group falls in the 'unradiogenic' domain of slab melts defined by Drummond *et al.* (1996) even if Antisana rocks are slightly richer in LILE than typical adakites. All these features argue against a strong contribution from the lower continental crust in the genesis of adakitic-like lavas of Antisana.

The OIB component?

Variations in the La/Nb ratio within the AND group suggest that a component rich in Nb is involved in the petrogenesis of these rocks. It has been proposed that Nb enrichment in lavas in subduction zone environments could be the consequence of a contribution from an ocean island basalt (OIB)-type mantle source (Reagan & Gill, 1989). The 'OIB component' assumption is reinforced by the presence of an alkaline volcano, Sumaco, 50 km east of Antisana volcano (Fig. 1).

There is no compelling evidence for extension in the back-arc region of the Northern Andes. On the contrary, there is strong evidence that compressive stresses dominate in this part of the arc (Ego *et al.*, 1996). Thus, the Sumaco alkaline lavas cannot be linked to the melting of an adiabatically uplifted mantle in an extensional setting. Should then Sumaco be related to an intracontinental hotspot? Barragan *et al.* (1998) analysed several rocks from Sumaco. These alkaline basaltic lavas are strongly enriched in LILE and contain modal haüyne and normative nepheline. The Sumaco lavas also clearly display negative Nb–Ta and Ti anomalies, which are an established characteristic of subduction-related lavas. Barragan *et al.* (1998) proposed that the Sumaco lavas could be generated by low degrees of partial melting of a mantle metasomatized by low inputs of slab-derived fluids. Thus, the Sumaco alkaline lavas should not be related to an intracontinental hotspot but seem to be derived from an enriched mantle source modified by a subduction component. This also rules out the involvement of an OIB-type source in the genesis of Antisana rocks.

Contribution of melts from the subducting oceanic crust

The occurrence of adakitic-like lavas at Antisana volcano and at other Ecuadorian volcanoes (Monzier *et al.*, 1997; Bourdon *et al.*, 2001) suggests that the AND group, which displays among the Antisana rocks the 'most adakitic' geochemical features (such as lowest HREE concentrations, highest La/Yb and Sr/Y ratios) could well be derived from direct partial melting of the subducting oceanic crust. However, there are many arguments against this assumption. Gutscher *et al.* (1999) estimated the slab to be at least 100 km deep under Antisana. This is too deep to be in the 'adakitic window' that predicts the melting of the oceanic crust to occur between 75 and 85 km (Drummond & Defant, 1990). Moreover, we have shown that the AND group differs in many ways from typical adakites. Lastly, Fig. 9 shows that high Ba/Nb ratios tend to be negatively correlated with Nb concentrations. If slab melts were directly involved in the petrogenesis of the AND group rocks, a positive correlation between Ba/Nb and Nb should be observed, as adakitic magmas are thought to transport Ba and Nb into the mantle wedge (Kesson & Ringwood, 1989). In

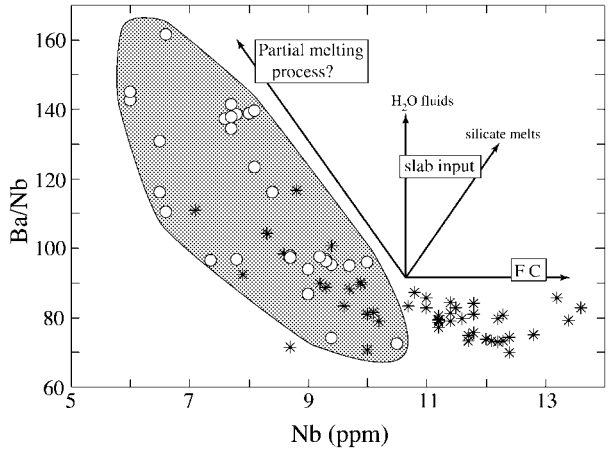

Fig. 9. Ba/Nb ratio vs Nb for the Antisana lavas. Theoretical fractional crystallization (FC), partial melting, hydrous fluids or silicate melts input trends are shown. Same symbols as in Fig. 6.

fact, an increasing influence from hydrous fluid metasomatism is not a viable hypothesis for the petrogenesis of either group. As Nb is supposed to be rather immobile in aqueous solutions (Tatsumi *et al.*, 1986; Tatsumi & Kogiso, 1997), Ba/Nb ratios should increase without significant variation in Nb concentration, which is also not observed. Another process is clearly driving this peculiar geochemical evolution.

Diminishing Yb concentrations correlated with increasing SiO_2 content is a well-known characteristic of amphibolite melting (Gill, 1981). It seems rather unusual, however, to generate rocks with SiO_2 contents as low as 53% from an amphibolitic source with realistic degrees of partial melting (Sen & Dunn, 1994; Rapp & Watson, 1995). The presence of these basic rocks is strong evidence that the dominant source of the Antisana magmas is in the mantle wedge rather than the subducting plate, whatever the contribution from the slab is.

It is important to note that all the Antisana rocks are characterized by a strong fractionation of HREE over the LREE. For example, La/Yb ratios range between 16 and 39 and the majority are above 20. Yb is also always lower than 1·8 ppm, which is very unusual for subduction-related rocks produced in the mantle. These features suggest that residual garnet ($\pm$ amphibole?) should be present in the source of all the Antisana rocks. Compared with adakites from the Western Cordillera, Antisana rocks are richer in HREE and Y and thus appear to be intermediate between true adakites and 'normal' calc-alkaline rocks. They also display high LILE contents typical of calc-alkaline lavas.

The intermediate characteristics of the Antisana rocks between adakites and mantle-derived melts suggest that the magmas result from the melting of a hybrid source that could be a depleted mantle metasomatized by slab melts. Wyllie & Sekine (1982) have experimentally shown that reaction between peridotite and K-rich silicic magma produces refertilized zones of hybridized mantle containing phlogopite, and Carroll & Wyllie (1989) further demonstrated that such reactions produce clinopyroxene, orthopyroxene, pargasitic hornblende and garnet. Prouteau *et al.* (2001) have experimentally shown that the interaction between adakite and peridotitic mantle rocks induces the consumption of mantle olivine. The presence of true adakites in the Western Cordillera (in a fore-arc position relative to Antisana volcano; Bourdon *et al.*, 2001) suggests that such a highly heterogeneous and enriched mantle could have been created at shallower depths and dragged down by mantle convection beneath Antisana volcano.

Figure 10 shows a MORB-normalized (Sun & McDonough, 1989) extended trace element diagram for four representative rocks from Antisana. The order of the elements has been arranged according to the degrees of enrichment expected in slab fluids, increasing from right to left (Maury *et al.*, 1992). As shown, each rock group displays a positive anomaly in Nb and other HFSE, suggesting an 'excess' of Nb compared with classical calc-alkaline rocks. This supports the assumption that the metasomatic agent that produced the source of Antisana rocks is a Nb-rich adakitic magma rather than a Nb-poor aqueous fluid. Moreover, Nb (and HFSE) enrichment in potassic calc-alkaline rocks (relative to less potassic rocks) has long been attributed to involvement of slab melts in their source (Ringwood, 1974; Wyllie & Sekine, 1982; Stolz *et al.* 1996). The depletion in HREE and Y shown by the Antisana rocks is consistent with such an assumption, as slab melts are also depleted in these elements (Defant & Drummond, 1990). Yogodzinski *et al.* (1994) have calculated that partial melting of a mixture of depleted mantle plus adakite produces magmas with mantle-normalized trace element patterns displaying negative Nb anomalies and moderate HREE depletion (e.g. Yb 0·9), which are consistent with the Antisana data. Of course, the Yogodzinski *et al.* (1994) calculation is oversimplified, as metasomatism of the mantle by adakitic magmas should give a range of compositions intermediate between a bulk mixture of the two reactants and selective enrichment that reflects ion exchange between the host mantle and the percolating liquid (Navon & Stolper, 1987; Nielson *et al.*, 1993). Bau & Knittel (1993) have shown that the geochemical characteristics of Mount Arayat basalts in the Philippines (varying La/Yb and Yb concentrations) could be explained by melting of such a highly heterogeneous domain. In the case of Antisana, it could also explain the slight geochemical variations in HREE between the AND group and the most primitive rocks from the CAK group (although evolution of the latter seems dominated by AFC).

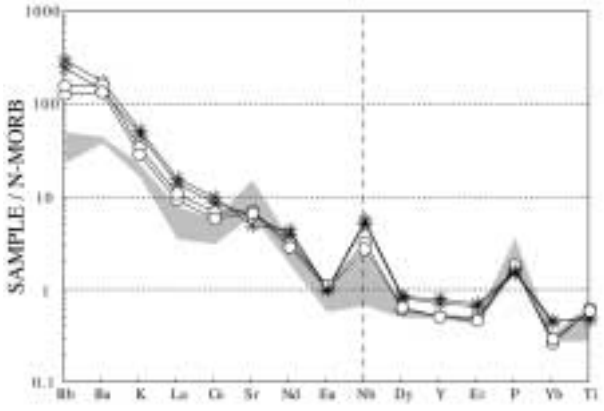

Fig. 10. Extended trace element plots for two CAK and AND representative lavas from Antisana volcano normalized to N-MORB of Sun & McDonough (1989). The order of the elements has been arranged according to the degree of enrichment expected in slab fluids, increasing from right to left (Maury *et al.*, 1992). Grey shaded field is for representative adakites from Zamboanga, Philippines (Sajona *et al.*, 1996). The strong positive Nb anomalies in the Antisana lavas and typical adakites should be noted. Same symbols as in Fig. 6.

Variations in La/Nb ratio and the unusual behaviour of Nb within the AND group suggest that a specific process affects the HFSE in the magma source. In many arc settings all over the world in which adakitic magmas are produced, and most exclusively in these special cases (Defant *et al.*, 1992), a peculiar type of magma called high-Nb basalt (HNB; Cascades arc, Leeman *et al.*, 1990) or Nb-enriched basalt (NEB; Philippines, Sajona *et al.*, 1994) has been recognized. The specific geochemical characteristics of these basic lavas led many workers to suggest that they were produced in an enriched mantle previously metasomatized by adakitic magmas (Defant *et al.*, 1992; Kepezhinskas *et al.*, 1996; Sajona *et al.*, 1996). This mantle has been proposed to contain HFSE-rich metasomatic minerals such as amphibole, phlogopite, ilmenite or rutile. In fact, these NEB or HNB magmas display different geochemical characterisitics depending on the arc. In the Cascade arc and Panama–Costa Rica, they are true basalts with particularly elevated contents of K_2O and, thus, belongs to the shoshonitic series (Leeman *et al.*, 1990; Defant *et al.*, 1992). In Zamboanga (Philippines), NEB are basalts or basic andesites with much lower concentrations of K_2O and LILE (Sajona *et al.*, 1996). Thus, it seems that mantle metasomatized by adakitic magmas is able to generate fairly silica-rich magmas.

Lavas of the AND group display a progressive enrichment in Nb towards the more basic members of the suite. These rocks represent a 'Nb-enriched group' among the Antisana rocks although they cannot be considered as typical Nb-enriched lavas. For example, among AND lavas, the La/Nb ratio has a minimum of 2·4 instead of 1·75 for the maximum value among typical high-Nb lavas from Zamboanga (Sajona *et al.*, 1996).

Nevertheless, similarly to Zamboanga lavas, correlated variations of Nb and Ti concentrations (not shown) in AND group suggest that a mineral phase controls the HFSE systematics in the Antisana magmas source. This phase could well be the result of interaction between adakitic magmas and the peridotitic mantle wedge (Kepezhinskas *et al.*, 1996). Nb anomalies in AND group mantle-normalized trace element patterns suggest that this phase is stable throughout the genesis of the series.

During progressive mantle partial melting, it has been shown that garnet is the first phase to be consumed (Mysen & Kushiro, 1977). This, and the fact that HFSE-retaining minerals and garnet are still present in the source of Antisana lavas suggest (1) high abundance of these phases in the source, (2) low degree of partial melting or (3) both.

Partial melting of a hybrid mantle metasomatized by slab melts

As shown above, fractional crystallization or direct partial melting of oceanic crust fails to explain the main geochemical variations among the Antisana rocks (between AND and CAK types, or within the AND group), and particularly the unusual behaviour of LILE vs Nb as well as LILE vs HREE in the AND group. There is, however, strong evidence that the AND group magmas are generated in the mantle wedge, mainly because of the presence of basic rocks, and that slab melts from the downgoing subducting plate are an important control of the genesis of the parental magmas. The independence of Nb from concentrations of other very incompatible elements suggests that a mineral phase retains this element in the source of the AND group. This could be either amphibole or ilmenite (Sajona *et al.*, 1996). The correlation between TiO_2 and Nb contents among the AND group lavas also suggests a residual Ti-rich phase. For HREE and Y, the residual phase is presumed to be garnet and/or amphibole. To evaluate the nature of the residual mineral phases in the mantle source, we model the trace element characteristics of the Antisana lavas.

Partial melting of a homogeneous mantle source with a fixed amount of a refractory HFSE or HREE-retaining phase leads to melts with the following characteristics: (1) abundances of LILE, alkalis and Ba, highly incompatible elements, are highest in melts derived by low degrees of partial melting; (2) ratios of these elements to the more compatible elements Nb and Yb (for example), which are retained by the accessory mineral, are highest in melts generated by low degrees of melting (e.g. Minster & Allègre, 1978). These predicted relationships correspond exactly to what is observed in the AND group lavas (Fig. 11).

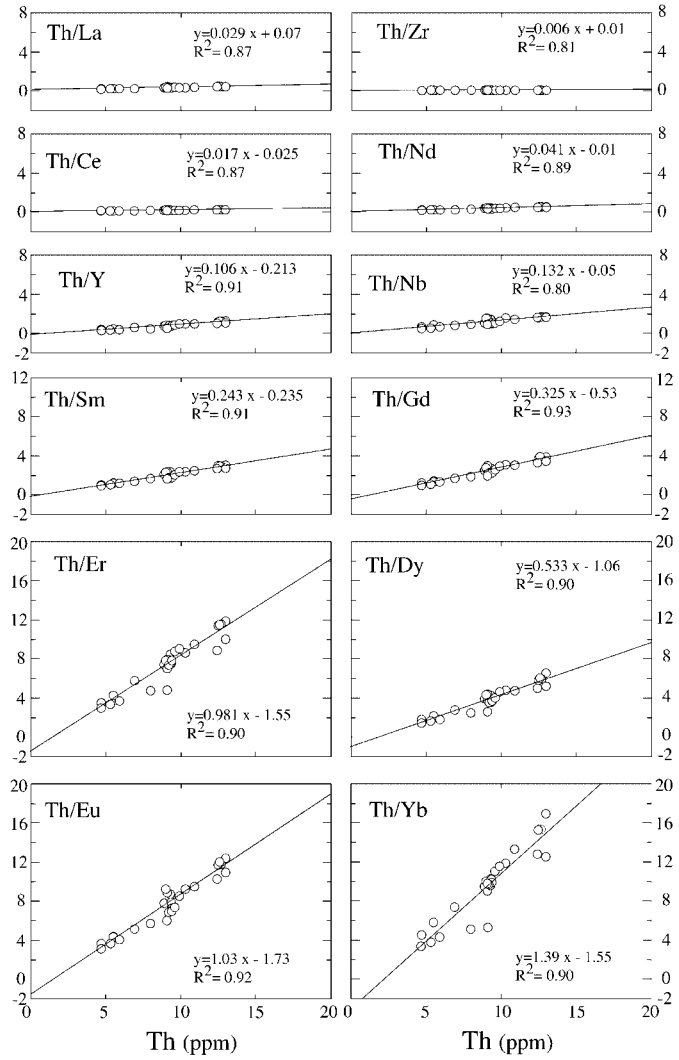

Fig. 11. Th/X vs Th diagrams, where element X is La, Ce, Y, Sm, Er, Eu, Zr, Nd, Nb, Gd, Dy and Yb. The slopes are related to the batch partial melting equation of Shaw (1970) as discussed in the text.

Although AND group lavas are probably not in equilibrium with typical mantle (mainly because of *mg*-number, and Ni and MgO contents, which are too low), we believe that AND group lavas could well be generated in a veined mantle metasomatized by slab melts. The constancy of *mg*-number, and FeO*/MgO and Nd/Sr ratios throughout the series suggests that it was not extensively affected by olivine, pyroxene or plagioclase fractionation.

Allègre & Minster (1978) showed that the ratio of the concentration of a highly incompatible element (H) to a moderately incompatible element (I) can be used to identify partial melting trends. In Fig. 11, AND data have been plotted in $C^{Th}/C^{element}$ vs C^{Th} diagrams, where C is the concentration of the element. In all diagrams, data plot on well-defined linear trends that, in view of preceding remarks, cannot be simply explained by a process other than batch partial melting. The correlation coefficients calculated for the corresponding linear regression lines are usually better than 0·9. The slope and intercept, relative to the batch partial melting equation of Shaw (1970), are (Minster & Allègre, 1978) as follows:

$$\text{Slope: } Ai = \{D_o^I - D_o^H[(1-P^I)/(1-P^H)]\}/C_o^I \quad (1)$$

$$\text{intercept: } Bi = [C_o^H(1-P^I)]/[C_o^I(1-P^H)] \quad (2)$$

where C_o^I and C_o^H are the concentration of element I and H in the source, D_o^I and D_o^H are the partition coefficient of I and H in the starting mineral assemblage, and P^I and P^H are the partition coefficient of I and H in the melting mineral assemblage

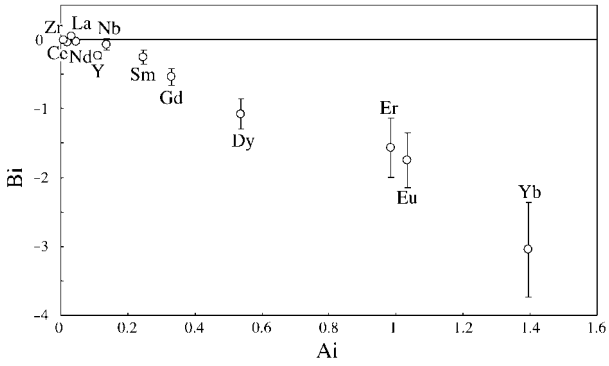

Fig. 12. ntercept (*Bi*) vs slope (*Ai*) diagram corresponding to the regression lines in Fig. 11. The respective standard deviations of the intercepts are also shown.

For a 'perfectly' incompatible element H (e.g. Th), P^H and D^H are close to zero and both parameters simplify to the following expressions:

$$\text{slope: } Ai = D_o^I / C_o^I \quad (3)$$

$$\text{intercept: } Bi = [C_o^H(1-P_l)] / C_o^I. \quad (4)$$

From (4), it becomes evident that when *Bi* is negative, $P^I > 1$; that is, a mineral with high K_d for element I is present in the source.

Bi values, with their standard deviations from the regression, have been plotted against the respective *Ai* values in Fig. 12. It can be concluded from the clear negative intercept of the HREE plots that garnet is probably present in the source of the AND group. Also, the negative intercept values for Sm, Eu and Gd imply that *P* values for these elements are greater than unity and that substantial amounts of amphibole and/or clinopyroxene with high K_d for MREE and Y are present in the source. The plot for Nb has a negative intercept but is close to zero, suggesting that *P* for this element is equal to or slightly greater than unity. This is also consistent with the presence of amphibole ($K_d^{Nb} = 1-1{\cdot}5$) in the source. Other incompatible elements display slope values close to zero, suggesting that $D_o^I \ll 1$ [see equation (3)] and thus a behaviour similar to that of Th during batch partial melting.

Following the evolution of LILE, the decreasing enrichment in silica and LILE from andesites to basic andesites among the AND group is compatible with increasing degree of batch partial melting. The correlated increasing concentrations in Nb, HREE and Y are also consistent with residual phases that become less stable as the degree of partial melting increases.

We have shown above that the high-Al andesites from the AND group could have existed in the crust as H_2O-rich magmas. This is consistent with the variable degrees of partial melting hypothesis to explain the unusual Antisana AND suite. If partial melting of metasomatized mantle is assumed to be linked to destabilization of metasomatic amphibole [following the model of Tatsumi (1986)], low concentrations of incompatible elements in high-Al andesites should correspond to high degrees of partial melting, i.e. higher amounts of destabilized amphibole (and thus higher amounts of H_2O in the melt). This would also explain the higher amount of Nb, primarily retained in this mineral phase, in the high-Al andesites.

Using incompatible element concentrations from Yogodzinski *et al.* (1994) for a depleted mantle metasomatized by adakitic magma, we have calculated that the range of incompatible element abundances from the less to the more evolved lavas of the AND group necessitates a variation of the degree of partial melting from 2% to 0·8%. These inferred low degrees of partial melting are consistent with the survival of residual garnet in the source of the Antisana magmas, as, with a larger amount of partial melting, garnet would be the first mineral to disappear.

Although it is clear that most andesites are not generated by partial melting of the upper mantle, but are derived from basaltic parents by fractional crystallization (Gill, 1981), there is some support for the idea that andesitic liquids can be produced directly in the mantle. Mysen & Boettcher (1975) obtained andesitic melts from the partial melting of hydrous peridotite; however, their results may have been influenced by modification of the melt upon quenching (Nicholls & Ringwood, 1974). More recently, Hirose (1997) obtained andesitic melts (54·4–60·3% SiO_2) by melting of the hydrous KLB1 natural lherzolite at relatively low temperature (1000–1050°C). He also showed that these melts contain >3% water, and lower FeO*, MgO and CaO contents compared with melts generated by partial melting of the same lherzolite at higher temperatures (Hirose & Kushiro, 1993). These results suggest that the production of primary andesitic melts in the mantle is possible, but only at relatively low temperatures.

One of the most interesting conclusions of Hirose (1997) is that the experimental melts generated contain >3% water. This could explain the subsequent evolution of the high-Al andesites where plagioclase fractionation may have been inhibited by the high water content of the parental magma (Sisson & Grove, 1993). Clearly, Hirose's (1997) results are not directly transposable to the Antisana case, as we envision a garnetiferous enriched mantle source, which is not the case for KLB-1. Nevertheless, if such a highly fertilized mantle exists beneath Antisana, its partial melting could produce andesitic melts similar to those erupted.

The intermediate MgO contents of the Antisana rocks strongly contradict their derivation as direct mantle melts. In Hirose's (1997) experiments, the MgO contents of the liquids reach 5·8–6·8%. Nevertheless, metasomatism of

the mantle by adakitic magmas is likely to be less efficient than by hydrous fluids. It may produce heterogeneously enriched domains, as proposed by Bau & Knittel (1993), composed of a highly veined mantle rich in metasomatic minerals, as observed in mantle xenoliths from the Kamchatka or Batan arcs (Kepezhinskas *et al.*, 1995; Schiano *et al.*, 1995). In this veined mantle, where olivine is no longer a dominant mineral of the assemblage (because it is consumed during slab melt–peridotite interaction), the hybrid enriched component should be the first to melt in later partial melting events (O'Reilly *et al.*, 1991; Foley, 1992), resulting in less mafic liquids than by partial melting of bulk hydrated peridotitic mantle.

CONCLUSIONS

Nd–Sr isotopic data for the Antisana volcanic rocks suggest a rather homogeneous mantle source that contrasts strikingly with the great variability observed for trace element ratios. This suggests that the petrogenesis of the most primitive lavas from both Antisana groups is dominated by mineralogical variations in the source rather than source geochemistry. The strong 'adakitic imprint' of the Antisana rocks suggests that they were generated in an enriched mantle that was heterogenously metasomatized by slab melts in a fore-arc position (i.e. beneath the Western Cordillera of Ecuador, where true adakites are erupted) and dragged down by mantle convection beneath the Eastern Cordillera. AND group petrogenesis seems dominated by variable degrees of partial melting of more enriched parts of this mantle, whereas the CAK group is dominated by fractional crystallization of a parental magma formed in a slightly less efficiently metasomatized part of the mantle. The peculiar behaviour of Nb suggests that an HFSE-rich mineral phase is controlling the partial melting process and that it could be metasomatic amphibole. Amphibole could also trigger directly partial melting by its destabilization once dragged down beneath the Antisana volcano after its formation in a fore-arc position beneath the Western Cordillera.

ACKNOWLEDGEMENTS

We deeply thank Chantal Bosq for carrying out the isotopic analyses. We thank Christian Coulon for helpful remarks, and Marc-André Gutscher for English improvements and stimulating discussions. Constructive reviews by Marc Defant, Jon Davidson and Chris Ballhaus greatly helped to improve the manuscript. We thank Marjorie Wilson for the final revision of this paper. This work forms part of E.B.'s Ph.D. financed by a grant from the French Ministry for Education, Research and Technology.

REFERENCES

Allègre, C. J. & Minster, J. F. (1978). Quantitative models for trace element behavior in magmatic processes. *Earth and Planetary Science Letters* **38**, 1–25.

Arculus, R. J. (1994). Aspects of magma genesis in arcs. *Lithos* **33**(1–3), 189–208.

Atherton, M. P. & Petford, N. (1993). Generation of sodium-rich magmas from newly underplated basaltic crust. *Nature* **362**, 144–146.

Barragan, R., Geist, D., Hall, M., Larson, P. & Kurz, M. (1998). Subduction controls on the compositions of lavas from the Ecuadorian Andes. *Earth and Planetary Science Letters* **154**, 153–166.

Bau, M. & Knittel, U. (1993). Significance of slab-derived partial melts and aqueous fluids for the genesis of tholeiitic and calc-alkaline island-arc basalts: evidence from Mt. Arayat, Philippines. *Chemical Geology* **105**, 233–251.

Bourdon, E., Eissen, J.-P., Cotten, J., Monzier, M., Robin, C. & Hall, M. L. (1999). Les laves calco-alcalines et à caractère adakitique du volcan Antisana (Equateur): hypothèse pétrogénétique. *Comptes Rendus de l'Académie des Sciences* **328**, 443–449.

Bourdon, E., Eissen, J.-P., Gutscher, M.-A., Monzier, M., Samaniego, P., Robin, C., Bollinger, C. & Cotten, J. (2001). Adakites and high-Mg andesites at Pichincha volcano (Ecuador): evidence for slab-melting and metasomatism beneath the Northern Andean Volcanic Zone. *Bulletin de la Société Géologique de France* (in press).

Brenan, J. M., Shaw, H. F., Phinney, D. L. & Ryerson, F. J. (1994). Rutile–aqueous fluid partitioning of Nb, Ta, Hf, Zr, U and Th: implications for high field strength element depletions in island-arc basalts. *Earth and Planetary Science Letters* **128**, 327–339.

Carroll, M. J. & Wyllie, P. J. (1989). Experimental phase relations in the system tonalite–peridotite–H_2O at 15 kbar, implications for assimilation and differentiation processes near the crust–mantle boundary *Journal of Petrology* **30**, 1351–1382.

Cotten, J., Le Dez, A., Bau, M., Caroff, M., Maury, R. C., Dulski, P., Fourcade, S., Bohn, M. & Brousse, R. (1995). Origin of anomalous rare-earth element and yttrium enrichments in subaerially exposed basalts: evidence from French Polynesia. *Chemical Geology* **119**, 115–138.

Davidson, J. P., McMillan, N. J., Moorbath, S., Worner, G., Harmon, R. S. & Lopez-Escobar, L. (1990). The Nevados de Payachata volcanic region (18°S/69°W, N. Chile) II. Evidence for widespread crustal involvement in Andean magmatism. *Contributions to Mineralogy and Petrology* **105**, 412–432.

Defant, M. J. & Drummond, M. S. (1990). Derivation of some modern arc magmas by melting of young subducted lithosphere. *Nature* **347**, 662–665.

Defant, M. J., Jackson, T. E., Drummond, M. S., De Boer, J. Z., Bellon, H., Feigenson, M. D., Maury, R. C. & Stewart, R. H. (1992). The geochemistry of young volcanism throughout western Panama and southeastern Costa Rica: an overview. *Journal of the Geological Society, London* **149**, 569–579.

DePaolo, D. J. (1981). Trace element and isotopic effects of combined wallrock assimilation and fractional crystallization. *Earth and Planetary Science Letters* **53**, 189–202.

Drummond, M. S. & Defant, M. J. (1990). A model for trondhjemite–tonalite–dacite genesis and crustal growth via slab melting: Archean to modern comparisons. *Journal of Geophysical Research* **95**(B13), 21503–21521.

Drummond, M. S., Defant, M. J. & Kepezhinskas, P. K. (1996). Petrogenesis of slab-derived trondhjemite–tonalite–dacite/adakite magmas. *Transactions of the Royal Society of Edinburgh: Earth Sciences* **87**(1–2), 205–215.

Ego, F., Sébrier, M., Lavenu, A., Yepes, H. & Egues, A. (1996). Quaternary state of stress in the Northern Andes and the restraining bend model for the Ecuadorian Andes. *Tectonophysics* **259**(1–3), 101–116.

Feeley, T. C. & Hacker, M. D. (1995). Intracrustal derivation of Na-rich andesitic and dacitic magmas: an example from volcàn Ollagüe, Andean Central Volcanic Zone. *Journal of Geology* **103**, 213–225.

Foley, S. (1992). Vein-plus-wall-rock melting mechanisms in the lithosphere and the origin of potassic alkaline magmas. *Lithos* **28**, 435–453.

Gill, J. G. (1981). *Orogenic Andesites and Plate Tectonics*. Berlin: Springer, 390 pp.

Gutscher, M.-A., Malavielle, J., Lallemand, S. & Collot, J. Y. (1999). Tectonic segmentation of the North Andean margin: impact of the Carnegie Ridge collision. *Earth and Planetary Science Letters* **168**, 255–270.

Harmon, R. S., Barreiro, B. A., Moorbath, S., Hoefs, J., Francis, P. W., Thorpe, R. S., Déruelle, B., McHugh, J. & Viglino, J. A. (1984). Regional O-, Sr-, and Pb-isotope relationships in late Cenozoic calc-alkaline lavas of the Andean Cordillera. *Journal of the Geological Society, London* **141**, 803–822.

Hawkesworth, C. J., Hammill, A. R., Gledhill, P. v. C. & Rogers, G. (1982). Isotope and trace element evidence for late-stage intra-crustal melting in the High Andes. *Earth and Planetary Science Letters* **58**, 240–254.

Hildreth, W. & Moorbath, S. (1988). Crustal contribution to arc magmatism in the Andes of central Chile *Contributions to Mineralogy and Petrology* **98**, 455–489.

Hirose, K. (1997). Melting experiments on lherzolite KLB-1 under hydrous conditions and generation of high-magnesian andesitic melts. *Geology* **25**(1), 42–44.

Hirose, K. & Kushiro, I. (1993). Partial melting of dry peridotites at high pressures: determination of compositions of melts segregated from peridotite using aggregates of diamond. *Earth and Planetary Science Letters* **114**, 477–489.

Hochstaedter, A. G., Kepezhinskas, P., Defant, M., Drummond, M. & Koloskov, A. (1996). Insights into the volcanic arc mantle wedge from magnesian lavas from the Kamchatka arc. *Journal of Geophysical Research* **101**(B1), 697–712.

Instituto Geográfico Militar (1993). Mapa Geologico de la Republica del Ecuador, 1/1.000.000^{e}, Quito

James, D. E. (1982). A combined O, Sr, Nd, and Pb isotopic and trace element study of crustal contamination in central Andean lavas, I. Local geochemical variations. *Earth and Planetary Science Letters* **57**, 47–62.

James, D. E. & Murcia, L. A. (1984). Crustal contamination in northern Andean volcanics. *Journal of the Geological Society, London* **141**, 823–830.

Kay, R. W. (1978). Aleutian magnesian andesites: melts from subducted Pacific ocean crust. *Journal of Volcanology and Geothermal Research* **4**, 117–132.

Kepezhinskas, P. K., Defant, M. J. & Drummond, M. S. (1995). Na metasomatism in the island-arc mantle by slab melt–peridotite interaction: evidence from mantle xenoliths in the north Kamchatka arc. *Journal of Petrology* **36**(6), 1505–1527.

Kepezhinskas, P. K., Defant, M. J. & Drummond, M. S. (1996). Progressive enrichment of island arc mantle by melt–peridotite interaction inferred from Kamchatka xenoliths. *Geochimica et Cosmochimica Acta* **60**(7), 1217–1229.

Kesson, S. E. & Ringwood, A. E. (1989). Slab–mantle interactions 1. Sheared and refertilized garnet peridotite xenoliths—samples of Wadati–Benioff zones? *Chemical Geology* **78**, 83–96.

Kuno, H. (1960). High-alumina basalt. *Journal of Petrology* **1**(2), 121–145.

Leeman, W. P., Smith, D. R., Hildreth, W., Palacz, Z. & Rogers, N. (1990). Compositional diversity of late Cenozoic basalts in a transect across the southern Washington Cascades: implications for subduction zone magmatism. *Journal of Geophysical Research* **95**(B12), 19561–19582.

Litherland, M., Aspden, J. A. & Jemelieta, R. A. (1994). *The Metamorphic Belts of Ecuador. British Geological Survey, Overseas Memoir* **11**, 147 pp.

Lopez-Escobar, L., Frey, F. A. & Vergara, M. (1977). Andesites and high-alumina basalts from the central–south Chile High Andes: geochemical evidence bearing on their petrogenesis. *Contributions to Mineralogy and Petrology* **63**, 199–228.

Maury, R. C., Defant, M. J. & Joron, J.-L. (1992). Metasomatism of the sub-arc mantle inferred from trace elements in Philippine xenoliths. *Nature* **360**, 661–663.

Maury, R. C., Sajona, F., Pubellier, M., Bellon, H. & Defant, M. (1996). Fusion de la croûte océanique dans les zones de subduction/collision récentes: l'exemple de Mindanao (Philippines). *Bulletin de la Société Géologique de France* **167**(5), 579–595.

Maury, R. C., Defant, M. J., Bellon, H., Jacques, D., Joron, J.-L., McDermott, F. & Vidal, P. (1998). Temporal geochemical trends in northern Luzon arc lavas (Philippines): implications on metasomatic processes in the island arc mantle. *Bulletin de la Société Géologique de France* **169**(1), 69–80.

McCulloch, M. T. & Gamble, J. A. (1991). Geochemical and geodynamical constraints on subduction zone magmatism. *Earth and Planetary Science Letters* **102**, 358–374.

Minster, J.-F. & Allègre, C. J. (1978). Systematic use of trace elements in igneous processes. Part III: inverse problem of batch partial melting in volcanic suites. *Contributions to Mineralogy and Petrology* **68**, 37–52.

Monzier, M., Robin, C., Hall, M. L., Cotten, J., Mothes, P., Eissen, J.-P. & Samaniego, P. (1997). Les adakites d'Equateur: modèle préliminaire. *Comptes Rendus de l'Académie des Sciences, Série IIa* **324**, 545–552.

Mysen, B. O. & Boettcher, A. L. (1975). Melting of a hydrous mantle, II. Geochemistry of crystals and liquids formed by anatexis of mantle peridotite at high pressures and high temperatures as a function of controlled activities of water, hydrogen and carbon dioxide. *Journal of Petrology* **16**(3), 549–593.

Mysen, B. O. & Kushiro, I. (1977). Compositional variations of coexisting phases with degree of melting of peridotite in the upper mantle. *American Mineralogist* **62**, 843–865.

Navon, O. & Stolper, E. (1987). Geochemical consequences of melt percolation: the upper mantle as a chromatographic column. *Journal of Geology* **95**, 285–307.

Nicholls, I. A. & Ringwood, A. E. (1974). Production of silica-saturated tholeiitic magmas in island arcs. *Earth and Planetary Science Letters* **17**, 243–246.

Nielson, J. E., Budahn, J. R., Unruh, D. M. & Willshire, H. G. (1993). Actualistic models of mantle metasomatism documented in a composite xenolith from Dish Hill, California. *Geochimica et Cosmochimica Acta* **57**, 105–121.

O'Reilly, S. Y., Griffin, W. L. & Ryan, C. G. (1991). Residence of trace elements in metasomatized spinel lherzolite xenoliths: a proton-microprobe study. *Contributions to Mineralogy and Petrology* **109**, 98–113.

Peacock, S. M. (1990). Numerical simulation of metamorphic pressure–temperature–time paths and fluid production in subducting slabs. *Tectonics* **9**(5), 1197–1211.

Peacock, S. M., Rushmer, T. & Thompson, A. B. (1994). Partial melting of subducting oceanic crust. *Earth and Planetary Science Letters* **121**(1–2), 227–244.

Peccerillo, P. & Taylor, S. R. (1976). Geochemistry of Eocene calc-alkaline volcanic rocks from the Kastamonu area, northern Turkey. *Contributions to Mineralogy and Petrology* **58**, 63–81.

Prouteau, G., Scaillet, B., Pichavant, M. & Maury, R. C. (2001). Evidence for mantle metasomatism by hydrous silicic melts derived from subducted oceanic crust. *Nature* **410**, 197–200.

Rapp, R. P., Watson, E. B. & Miller, C. F. (1991). Partial melting of amphibolite/eclogite and the origin of Archean trondhjemites and tonalites. *Precambrian Research* **51**, 1–25.

Rapp, R. P. & Watson, E. B. (1995). Dehydration melting of metabasalt at 8–32 kbar: implications for continental growth and crust–mantle recycling. *Journal of Petrology* **36**(4), 891–931.

Reagan, M. K. & Gill, J. B. (1989). Coexisting calc-alkaline and high-niobium basalts from Turrialba volcano, Costa Rica: implications for residual titanates in arc magma sources. *Journal of Geophysical Research* **94**(B4), 4619–4633.

Ringwood, A. E. (1974). The petrological evolution of island arc systems. *Journal of the Geological Society, London* **130**, 183–204.

Sajona, F. G., Bellon, H., Maury, R. C., Pubellier, M., Cotten, J., & Rangin, C. (1994). Magmatic response to abrupt changes in geodynamic settings: Pliocene–Quaternary calc-alkaline and Nb-enriched lavas from Mindanao (Philippines). *Tectonophysics* **237**, 47–72.

Sajona, F. G., Maury, R. C., Bellon, H., Cotten, J. & Defant, M. (1996). High field strength element enrichment of Pliocene–Pleistocene Island arc basalts, Zamboanga Peninsula, western Mindanao (Philippines). *Journal of Petrology* **37**(3), 693–726.

Saunders, A. D., Rogers, G., Marriner, G. F., Terrell, D. J. & Verma, S. P. (1987). Geochemistry of Cenozoic volcanic rocks, Baja California, Mexico: implications for the petrogenesis of post-subduction magams. *Journal of Volcanology and Geothermal Research* **32**, 223–245.

Schiano, P., Clocchiatti, R., Shimizu, N., Maury, R. C., Jochum, K. P. & Hofmann, A. W. (1995). Hydrous, silica-rich melts in the sub-arc mantle and their relationship with erupted arc lavas. *Nature* **377**, 595–600.

Sen, C. & Dunn, T. (1994). Dehydration melting of a basaltic composition amphibolite at 1·5 and 2·0 GPa: implications for the origin of adakites. *Contributions to Mineralogy and Petrology* **117**, 394–409.

Shaw, D. M. (1970). Trace element fractionation during anatexis. *Geochimica et Cosmochimica Acta* **34**, 237–243.

Sisson, T. W. (1991). Field, geochemical and experimental studies of aluminous arc magmas. Ph.D. thesis, MIT, Cambridge, MA.

Sisson, T. W. & Grove, T. L. (1993). Temperatures and H_2O contents of low-MgO high-alumina basalts. *Contributions to Mineralogy and Petrology* **113**, 167–184.

Stern, C. R. & Kilian, R. (1996). Role of the subducted slab, mantle wedge and continental crust in the generation of adakites from the Andean Austral Volcanic Zone. *Contributions to Mineralogy and Petrology* **123**, 263–281.

Stern, C. R., Futa, K. & Muehlenbachs, K. (1984). Isotope and trace element data for orogenic andesites from the Austral Andes. In: Harmon, R. S. & Barreiro, B. A. (eds) *Andean Magmatism: chemical and isotopic constraints*. Cheshire: Shiva Publishing, pp. 31–46.

Stolz, A. J., Jochum, K. P., Spettle, B. & Hofmann, A. W. (1996). Fluid- and melt-related enrichment in the subarc mantle: evidence from Nb/Ta variations in island-arc basalts. *Geology* **24**(7), 587–590.

Sun, S.-S. & McDonough, W. F. (1989). Chemical and isotopic systematics of oceanic basalts: implications for mantle composition and processes. In: Saunders, A. D. & Norry, J. M. (eds) *Magmatism in Oceanic Basins. Geological Society, London, Special Publications* 42, 313–345.

Tatsumi, Y. (1986). Formation of volcanic front in subduction zones. *Geophysical Research Letters* **13**(8), 717–720.

Tatsumi, Y. & Kogiso, T. (1997). Trace element transport during dehydration processes in the subducted oceanic crust: 2. Origin of chemical and physical characteristics in arc magmatism. *Earth and Planetary Science Letters* **148**(1–2), 207–222.

Tatsumi, Y., Hamilton, D. L. & Nesbitt, R. W. (1986). Chemical characteristics of fluid phase released from a subducted lithosphere and origin of arc magmas: evidence from high-pressure experiments and natural rocks. *Journal of Volcanology and Geothermal Research* **29**, 293–309.

Thorpe, R. S., Francis, P. W., Hammill, M. & Baker, M. C. W. (1982). The Andes. In: Thorpe, R. S. (ed.) *Andesites*. New York: Wiley, pp. 187–205.

Van Andel, T. H., Heath, G. R., Malfait, B. T., Heinrichs, D. F. & Ewing, J. I. (1971). Tectonics of the Panama Basin, Eastern Equatorial Pacific. *Geological Society of America Bulletin* **82**, 1489–1508.

White, W. M., McBirney, A. R. & Duncan, R. A. (1993). Petrology and geochemistry of the Galapagos islands: portrait of a pathological mantle plume. *Journal of Geophysical Research* **98**(B11), 19533–19563.

Wyllie, P. J. & Sekine, T. (1982). The formation of mantle phlogopite in subduction zone hybridization. *Contributions to Mineralogy and Petrology* **79**(4), 375–380.

Wyllie, P. J. & Wolf, M. B. (1993). Amphibole dehydration-melting: sorting out the solidus. In: Prichard, H. M., Alabaster, T., Harris, N. B. W. & Neary, C. R. (eds) *Magmatic Processes and Plate Tectonics. Geological Society, London, Special Publication* **76**, 405–416.

Yogodzinski, G. M. & Kelemen, P. B. (1998). Slab melting in the Aleutians: implications of an ion probe study of clinopyroxene in primitive adakite and basalts. *Earth and Planetary Science Letters* **158**, 53–65.

Yogodzinski, G. M., Volynets, O. N., Koloskov, A. V., Seliverstov, N. I. & Matvenkov, V. V. (1994). Magnesian andesites and the subduction component in a strongly calc-alkaline series at Piip volcano, Far Western Aleutians. *Journal of Petrology* **35**(1), 163–204.